Advances in Science and Technology Research Journal

Advances in Science and Technology Research Journal 2022, 16(5), 250–260
https://doi.org/10.12913/22998624/154895
ISSN 2299-8624, License CC-BY 4.0

Received: 2022.07.30
Accepted: 2022.10.17
Published: 2022.11.01

Strategies of Heating and Hardening External Corners on the Example of Bending Tools for Press Brakes

Irena Nowotyńska[1*], Stanisław Kut[1]

[1] Rzeszów University of Technology, Al. Powstańców Warszawy 12, 35-959 Rzeszów, Poland

* Corresponding author's e-mail: i_nowot@prz.edu.pl

ABSTRACT

In the paper the methods of laser hardening of external tool corners on the example of bending tools for press brakes were presented. The disadvantages and limitations of the most commonly used techniques for guiding a hardening laser light beam are presented, i.e.: (i) in one pass parallel to the tool corner plane symmetry, (ii) in two passes perpendicular to the surfaces adjacent to the corner, and (iii) in one pass perpendicular to the surface adjacent to the corner by using two diode lasers. The microstructure of the tool material after laser and induction hardening was compared. A significant influence of the heating method on the microstructure of the tool material after hardening was demonstrated. The original method of hardening the outer corners of bending tools using a hardening laser beam splitter was subject to a more detailed analysis. The analysis of material heating in simultaneously hardened corner area and adjacent surfaces was carried out using the Marc/Mentat software based on the finite element method. By analyzing the temperature distributions it was shown that if a beam splitter was used, obtaining a continuous and uniform hardened layer (i.e. with comparable hardness, depth, without tempered or non-tempered areas) in the area of the outer corner and adjacent surfaces was possible. In practice, achieving such a layer is conditioned by the correct selection of the size of the k parameter which determines the distance between the separated beams of laser light. Depending on the geometry of the hardened tool corner and the parameters of the hardening laser beam, this distance can be determined experimentally or on the basis of numerical simulation.

Keywords: bending tools, laser hardening, temperature distributions, FEM simulation

INTRODUCTION

Due to its properties, the laser beam is widely used as a heat source during various types of surface treatment of materials, in particular for surface laser hardening, cutting and laser welding of various types of structural elements including tools [1-3]. In the paper [1] a detailed investigation of the influence of laser parameters on the microstructure, phase and residual stress and mechanical properties of AISI H13 tool steel was carried out. In turn, in work [2] an attempt was made to improve the surface hardness and wear properties of AISI H13 tool steel through solid solution hardening and refinement of microstructures using a 200 W fiber laser as a heat generating source. Based on the survey obtained one can conclude that the hardening depth and width are increased with the growth in the heat input applied. In the paper [3], the effect of laser overlap on the low-carbon and stainless steel were investigated. The analyzed samples were made of AISI 4130 low-carbon steel and AISI 410 stainless steel with 50% overlap. In turn, in [4] an attempt was made to optimize the distance between successive paths, when the dimensions of the treated surface are larger than the cross-section of the laser beam. Slatter et al. [5] used a laser to treat the valve seat area of a cast iron cylinder head and carried out to investigate the fundamental wear characteristics of untreated cast iron and also cast iron with a range of laser treatments. In study [6] authors studied the effect of different types of tool textures, produced by nanosecond fibre laser, on the tribological conditions at the interface tool-formed material. The effect of the laser radiation

on the material depends primarily on the type of material, radiation length, radiation power density and the time of radiation exposure to the material. Physical phenomena occurring during the heating of various materials with a laser beam are described in [7]. The use of laser hardening enables machining of parts that could not previously be hardened by other methods [8]. In addition, it eliminates a number of difficulties that occur during induction hardening. It enables hardening of individual tool surfaces, most often the ones that are in contact with the workpiece and are exposed to pressure and abrasive wear [9]. In the case of laser hardening, it is possible to surface harden not only individual surfaces, but even their designated areas to the required depth and hardness, which allows obtaining hardened layers, harder with a finer-grained structure, thinner, static and fatigue resistant ,and the ones which are more resistant to abrasive wear. The advantage of laser hardening, compared to induction hardening, is that there is no need for finishing, e.g. grinding [10]. In addition, hardening of only selected tool surfaces reduces significantly the formation of hardening stresses, which are the cause of permanent tool deformations after hardening. Therefore, in practice, using laser hardening can minimize the hardened surface of the tool. This way one can practically reduce or eliminate permanent tool deformations after hardening.

Unlike other hardening techniques, laser hardening is based on a precise, localized heat source that produces extremely high intensities ideal for fast cooling and excellent hardening quality [11]. In this technique, obtaining the required hardness while minimizing thermal deformation is crucial as tools require high precision [12]. Unfortunately, it is a difficult task to meet the requirements for hardness and deformation, and a good predictive model can significantly reduce time and costs in finding optimal process conditions that may or may not actually exist [13]. For this reason, extensive research was carried out to develop predictive models or to discover the relationship between process parameters and process results [14-16]. In [14] a theoretical and experimental study of heat flow and solid-state phase transformations during the laser surface hardening of 1018 steel was conducted. Whereas in the paper [15] an analytical solution for the temperature rise distribution in laser surface transformation hardening of a steel workpiece of finite width is developed based on classical moving heat source method to predict the optimal operational parameters. Also an exact solution was developed for a quasi-steady-moving-interface heat transfer problem in laser transformation hardening by a beam customized to a flat-top rectangular shape [16].

Fortunato et al. [17] developed a mathematical model for the simulation of hardening by means of laser transformation of hypo-eutectoid carbon steels. Focusing on developing a simple model to reduce computation time, they calculated 3D thermal fields and predicted the evolution of microstructures. In the study [18], a finite element method is presented with an aim to predict the temperature distribution for optimizing laser surface hardening process on a cylindrical steel solid rod. Martinez et al. [19] studied hardening using scanning optics. To control the process temperature, numerical simulations were used to minimize the experimental work required to develop a closed-loop temperature control system. Lambiase et al. [20] developed an artificial neural network to predict the hardness of laser hardened steels. The temperature history calculated using the 1-D analytical model was used for their model. Knap et al. [21] studied the effect of chemical composition on hardenability within one steel grade, with broad and heterogeneous data used to predict hardness. They found that by focusing on a narrow process region, neural network models were able to accurately predict hardness based on chemical composition. In [22], a 3-D thermal analysis assisted by a systematic experimental study using a 2 kW multi-mode fiber laser was employed to develop predictive models for hardness and thermal deformation in laser transformation hardening of AISI H13 tool steel. In turn in [23] a mathematical model has been developed to calculate the temperature distribution on the surface and bulk of a steel plate under the laser hardening process. The model starts from the basic heat equation, is then developed to a volumetric form and is connected to the various solid phases existing. The model is based on two strongly influencing parameters of the laser hardening process: velocity of the laser spot and irradiation time.

The formation of permanent deformations after hardening is one of the biggest technological problems in the production of tools for press brakes and folding machines. Their length can be up to 4000 mm and more, while the required straightness deviation over the length of one meter of the tool is in practice about 10 micrometers.

In industrial practice, obtaining the required straightness is a big challenge for manufacturers of this type of tool, which explains the growing popularity of laser hardening methods.

However, the laser hardening method, despite many advantages, has its disadvantages and limitations, among others [24] it is impossible to overlap hardening traces because in the common area there is a phenomenon of reduced hardening hardness due to double tempering, and the minimum distance of hardening traces is about 1.0–1.5 mm, hardening of larger surfaces involves covering this area with parallel or meandering hardening paths, depending on the optical system used, the distance between the laser head and the workpiece is from approx. 100–350 mm, the need to guarantee free access of the laser head to the workpiece.

In the paper there was presented a new original technique of laser hardening [25] of the outer corners of bending tools by means of a laser beam splitter against the background of previously known hardening techniques, whose disadvantages and limitations were specified. In order to demonstrate the impact of the k parameter (characteristic of the new method and characterized later in the article) on the effectiveness of the new laser hardening technique, a numerical analysis of the heating process of a tool with a given geometry was carried out using different values of this parameter. By analyzing the temperature distribution fields, it was shown that the value of the k parameter had the significant impact on the parameters of the hardened layer.

METHODS OF LASER HEATING

Currently, various laser hardening techniques are used in practice. In the case of bending tools, only the corner and adjacent surfaces of a certain length are most often hardened. This length depends on the size of the contact surface of the shaped material with the tool. Several methods of laser hardening of tools are known to date in terms of aligning and guiding a laser beam with respect to hardened tool surfaces. The first of these is shown in Figure 1. It consists in the fact that the beam of hardening laser light with the B width is directed at the tool so that the central part of the beam falls on the corner parallel to its plane of symmetry. In this way, it heats the corner and part of the surfaces adjacent to it at lengths L1 and L2. The lengths L1 and L2 of hardened surfaces depend on the angle of inclination of surfaces adjacent to the corner α_1 and α_2 and are respectively:

$$L1 = B/2\ sin(\alpha_1) \tag{1}$$

$$L2 = B/2\ sin(\alpha_2) \tag{2}$$

In the case when the angles of the surfaces adjacent to the corner are the same $\alpha_1 = \alpha_2$, then L1 = L2. However, if the angle $\alpha_1 < \alpha_2$, then L1 > L2. The smaller the tip angle of the tool, the larger the tool surface is hardened assuming a constant beam width. The advantage of this method is that the required surfaces are hardened simultaneously in one pass of the hardening laser light beam. However, this solution has several disadvantages. One of them is that the light beam does not fall perpendicular to the hardened tool, which significantly reduces the heating efficiency. In addition, if the angle $\alpha_1 \neq \alpha_2$, then the individual adjacent surfaces are not heated equally, and this causes that their properties after hardening are not the same. In this type of method, the length of hardened sections L1 and L2 on the surfaces adjacent to the corner is a serious limitation. In most cases, it is insufficient, especially at larger tool angles. In the case where the presented hardening method cannot be used due to the insufficient length L1 and L2, the hardening technique shown in Figure 2 is applied.

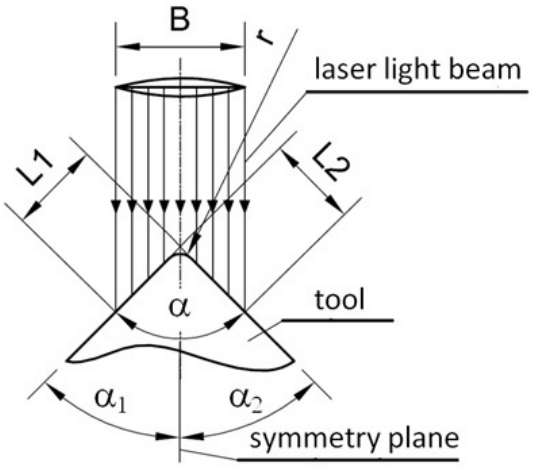

Fig. 1. The way of setting and guiding the beam of hardening laser light during hardening of the corner and adjacent surfaces in one pass

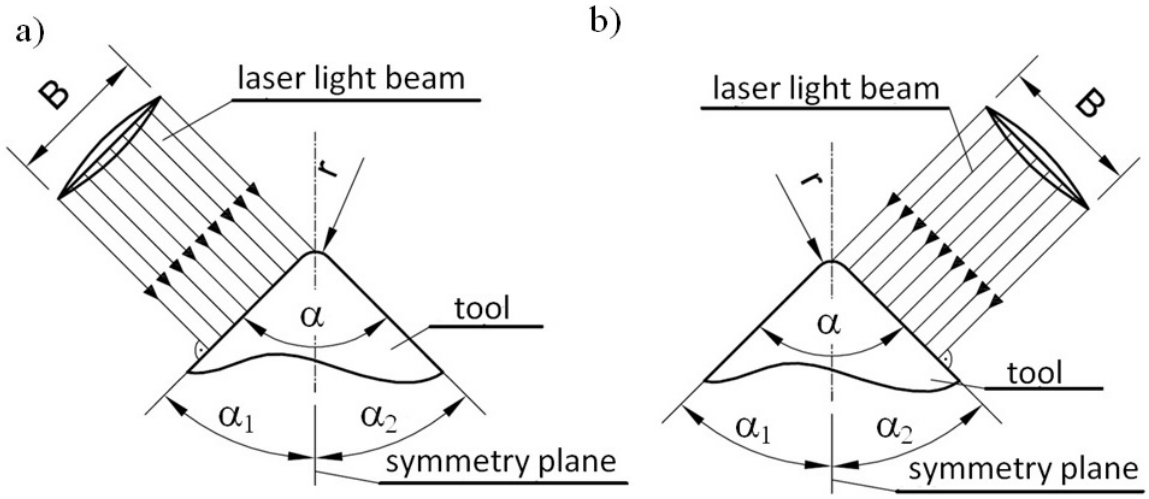

Fig. 2. The way of setting and guiding the beam of hardening laser light during hardening of the corner and adjacent surfaces in two passes: a) first pass, b) second pass

In the first pass, shown in Figure 2a, part of the corner and one adjacent surface are hardened, in the second pass (Fig. 2b), the remaining part of the corner and the second adjacent surface are hardened. This approach allows full coverage of the hardened layer of adjacent surfaces of the required length L1 and L2 equal to the width B of the hardening laser beam. Also in this case, the heating efficiency is much higher than in the previous method shown in Figure 1, because the laser light falls on the surfaces adjacent at right angles. An important disadvantage of this solution is that on the surface of the corner of the tool, at the very tip, a tempered or non-hardened area is created. This is a disadvantage as the bending tool in this place is the most loaded during operation. This defect can hardly be eliminated. If the light beam in the second pass is close to the area already hardened in the first pass, it will heat this area partially, as a result of which the material in this area will be tempered. On the other hand, if the beam of the hardening laser light in the second pass is moved away from the hardened area in the first pass, it will create an unhardened area between the hardened ones. In the method of hardening with the use of two hardening lasers shown in Figure 3, the light beams of the first laser with a width of B1 and the second laser with a width of B2 simultaneously heat all adjacent hardened surfaces.

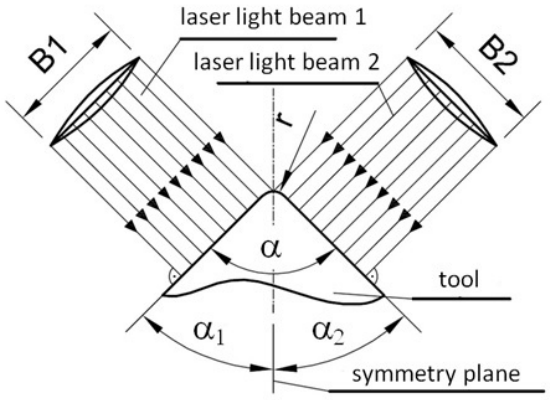

Fig. 3. The method of hardening by means of two lasers

This solution, however, almost doubles the cost of the hardening device by the need for a second hardening laser, but this is not a technical limitation in the practical application of this method. The limitation, however, results from the fact that it is practically impossible to select two lasers with the same real power and thus heating characteristics. For this reason, the properties of individual surfaces will always vary after such hardening.

In order to eliminate the presented disadvantages resulting from the application of the hitherto known methods of laser hardening, an original method of hardening with laser beam distribution was developed using a light beam splitter enabling the practical application of this technique for hardening tools, especially bending tools.

This method consists in splitting the light beam 6 of a hardening laser into two symmetrical 7 and 8 (Fig. 4a) or asymmetrical 9 and 10

(Fig. 4b) light beams and using a set of mirrors 1–4 directing them (preferably at a right angle) to tool surfaces 5 to be hardened. Both during heating with symmetrical and asymmetrical distribution, the separated light beams 7 and 8 of the hardening laser should fall on the tool 5 so as not to cover the apex itself over a certain width k depending on the heating parameters. It is beneficial if the very tip of the tool with a width of k is heated as a result of heat penetration into it when heating the surfaces adjacent to it. If the laser light covers the entire corner of the tool (including the surface with a width of k), its temperature after heating will be higher than other surfaces after heating, and this will cause uneven distribution of hardness and depth of the layer after hardening.

Thanks to the use of a laser beam splitter, it is possible to simultaneously heat the corner and adjacent surfaces at the desired width in one pass with the same parameters, which positively affects the material properties in the hardened area of the tool and is more economical.

EXPERIMENTAL RESEARCH

The purpose of experimental research was to compare the material properties in the hardened area of the bending die (Fig. 5) using the laser hardening and induction hardening techniques. Induction hardening is a conventional technology for surface hardening of tools and more. Despite the difficulties associated with the necessity of grinding surfaces after induction hardening, the inability to harden individual surfaces or their parts, the occurrence of permanent deformations, especially when hardening long products and with variable cross-sections or obtaining the same thickness of hardened layer, is widely used in industry also in the production of bending tools.

The die tested was made of tool steel grade 1.2312 (40CrMnMoS8-6) with the composition given in Table 1 was subject to conventional induction hardening and laser hardening at 860°C. Laser hardening was carried out using the LDF 4000-60 diode laser with 4400 W power and wavelength (980–1020) nm (Fig. 6).

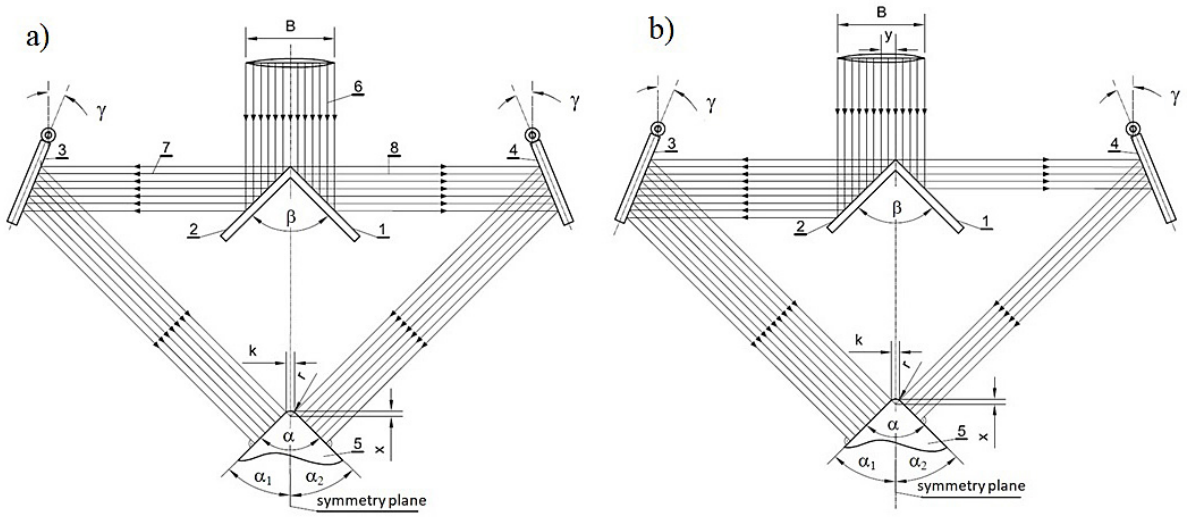

Fig. 4. Methods of setting and guiding the laser beam during hardening using a laser beam splitter: a) symmetrical, b) asymmetrical

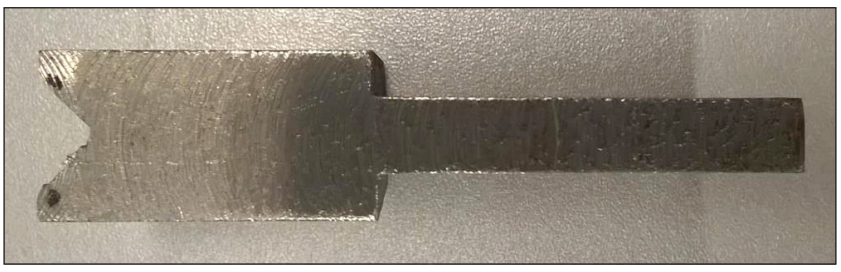

Fig. 5. Shape of the tested bending tool

Table 1. Chemical composition of the die material tested

C	Si	Mn	P	S	Cr	Mo	W	V	Co	Ni
0.35–0.45	0.30–0.50	1.40–1.60	Max 0.030	0.050–0.100	1.80–2.00	0.15–0.25	–	–	–	–

In order to determine the impact of hardening on the material properties in the hardened area of the bending die, microstructure tests and hardness measurements were performed by means of laser hardening and induction hardening techniques. Observations of the microstructure were carried out using a Leica DMI 3000M metallographic light microscope. Two samples (cross-sections made through hardened layer), after laser hardening and after induction hardening, were tested. Based on the tests, the microstructure of the samples in the surface zone and in the transition zone was revealed (Fig. 7). In the tool after laser hardening, the martensitic structure and ferrite grains are visible in the surface strip, while in the transition zone the bainite grains (upper and lower) and ferrite grains are visible. Martensitic layer provides hardness and abrasion resistance of the surface layer of the element. The transition layer, however, remains less durable but more ductile. In turn, in a sample processed by induction, a martensitic structure can be observed in the surface area, which reaches much deeper than in the case of laser hardening. In the transition area, bainite and ferrite can be seen in the induction hardened tool.

Hardness measurement was carried out using the Vickers method ($HV_{0.3}$) at 3N (0.3 kG) load. During the measure the NEXUS 4303 microhardness test was used. Several paths were made for each sample (Fig. 8) starting from a distance of 0.1 mm from the surface, each subsequent impression was made at a distance of 0.2 mm from the previous one.

The hardness distribution in a laser and induction hardened sample in three measuring zones for each sample is shown in Figure 9.

The hardness measurement values in the areas marked as 1_1 and 2_1 (Fig. 9a) corresponding to laser and induction hardening, respectively and located in horizontal parts of the bending tool differ from each other almost twice, especially to a depth of about 3 mm. Higher hardness values were recorded for induction hardened samples. In the case of measuring areas (1-2 and 2-2) located near the corner of the tool, the maximum hardness values are almost the same and oscillate around a value of 600 $HV_{0.3}$ (Fig. 9b). In the case of laser hardening, the highest hardness value was recorded right at the surface, as it goes deeper into the sample, the hardness decreases to about 200 $HV_{0.3}$ at a depth of about 1.5 mm. The hardness distribution in the induction hardened sample looks different, due to the larger hardening range, the hardness value remains almost at one level assuming a value of 600 $HV_{0.3}$. For the measuring area (1-3 and 2-3) lying on the tool plane, the highest hardness values were recorded for the areas 1-3, at the surface which corresponds to the sample after laser hardening and is over 700 $HV_{0.3}$ and is more

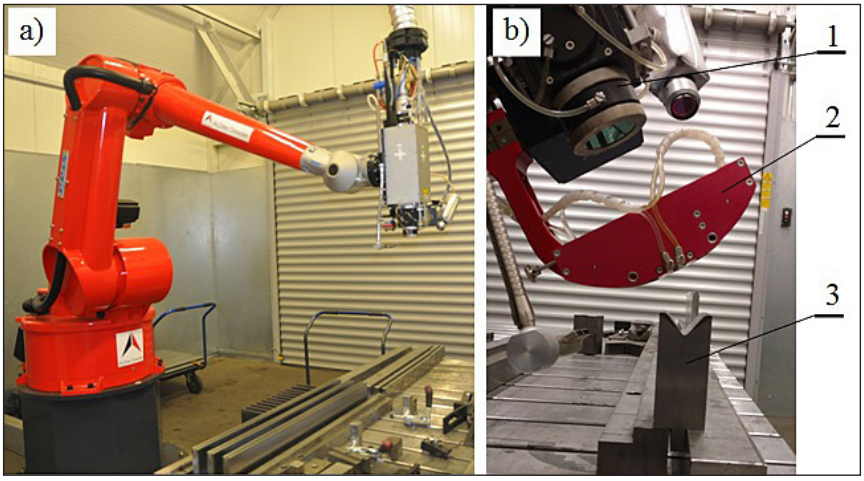

Fig. 6. Testing station for diode laser hardening: a) general view, b) 1 – optical system, 2 – beam splitter, 3 – sample (PPMiU PLASMET Sp.z o.o.proprietary)

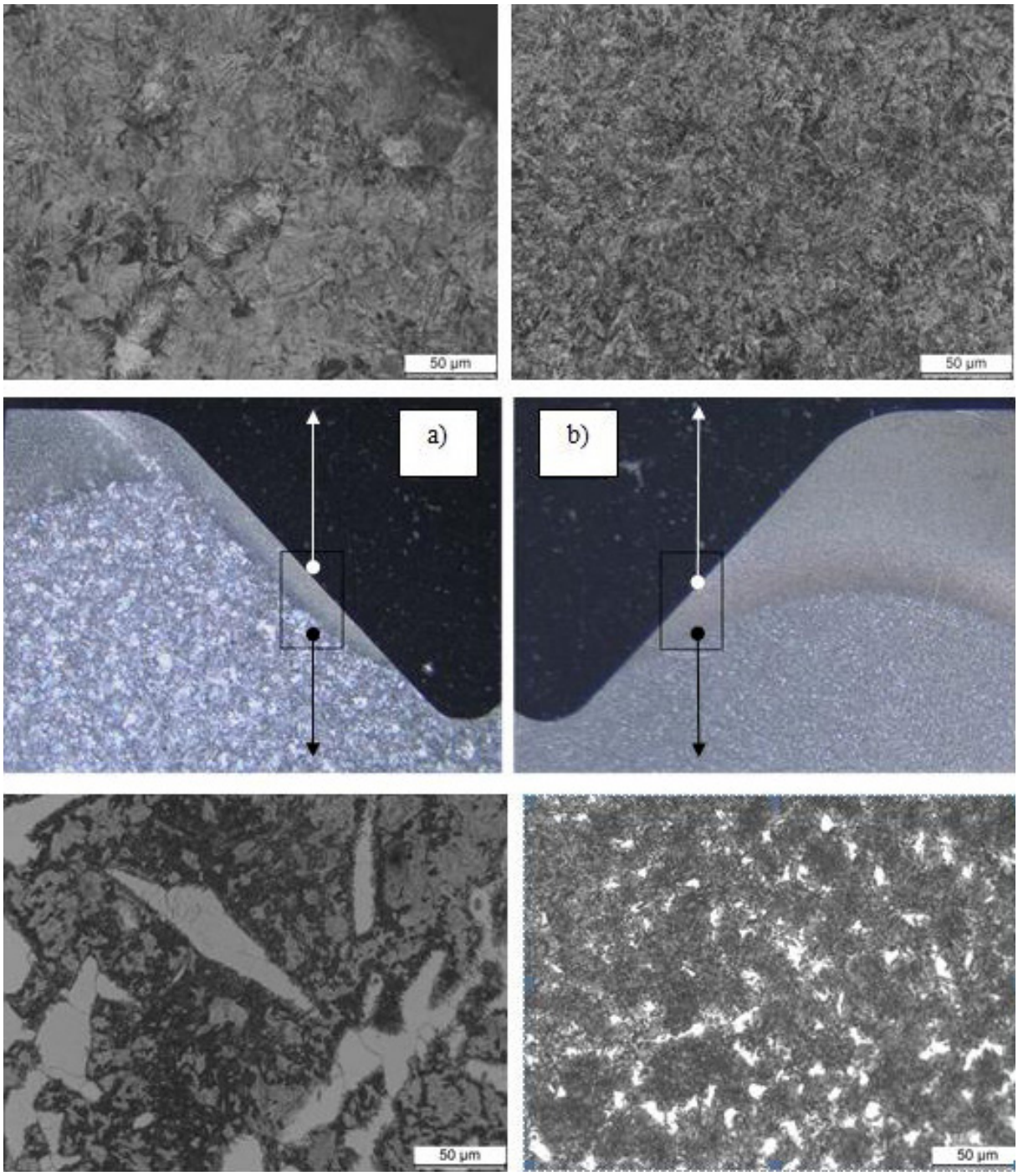

Fig. 7. Microstructure of samples in the surface layer and in the transition layer: a) after laser hardening, b) after induction hardening

than 200 $HV_{0.3}$ higher than the hardness recorded for this depth for the sample after induction hardening. Positive effects of laser hardening can be observed here, which ensures high hardness of the tool to a depth of about 1.5 mm, while the remaining area is more ductile and resistant to high loads. In turn, after induction hardening, a lower hardness on the surface was obtained with a large depth of the hardened layer, which may result in the tool being less durable during operation.

AN ANALYSIS OF EXTERNAL CORNER HEATING

As already mentioned in the laser hardening method using a beam splitter, the characteristic parameter affecting the quality of the hardened layer in the area of the corner and adjacent surfaces is the k parameter shown in Figure 4. To determine the significance of the impact of this parameter on the quality of the hardened layer,

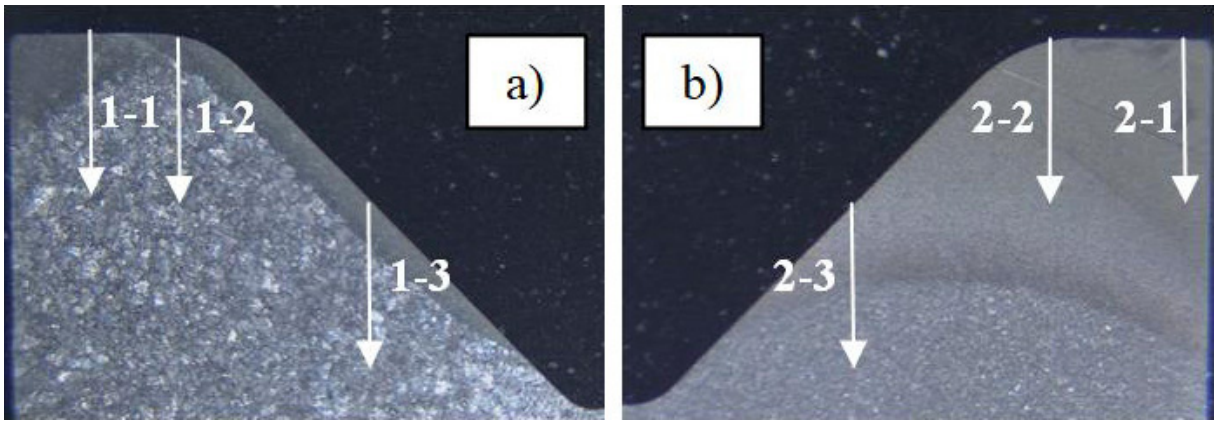

Fig. 8. Places of hardness measurement: a) after laser hardening, b) after induction hardening

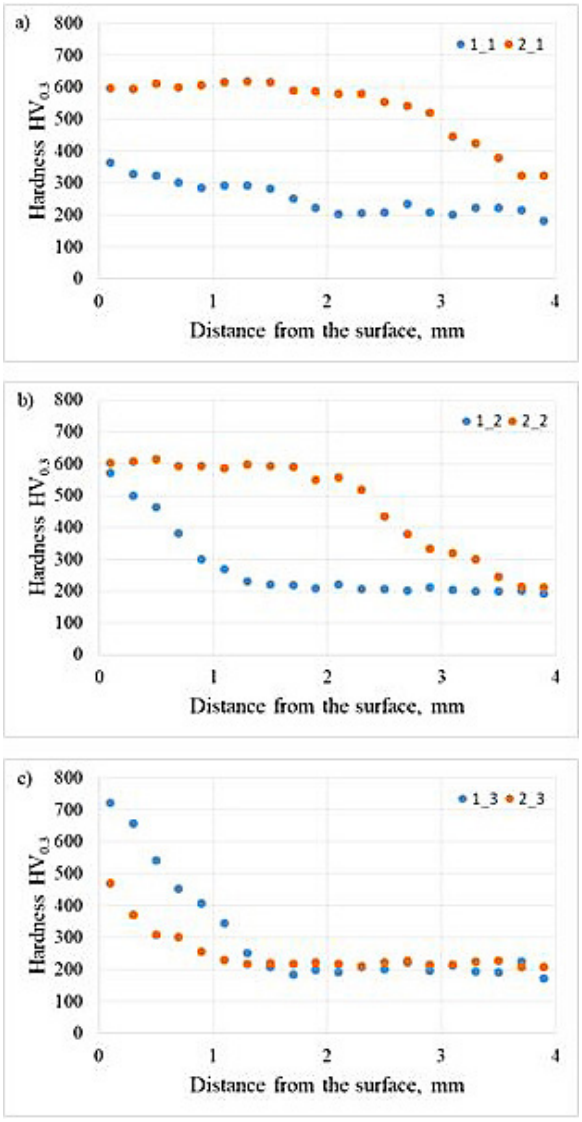

Fig. 9. Hardness distribution in three measuring zones in a laser-hardened sample (blue points) and in an induction-hardened sample (red points)

numerical simulation of the process of heating tool surfaces subject to hardening was done. A typical bending punch for press brakes was selected for testing (Fig. 10). With this tool, the outer corner 1 and the adjacent surfaces 2 and 3 are subject to surface hardening for a given length.

The numerical model of the heating process was built in the MARC/Mentat system for the part of the tool where hardening is carried out. In order to perform thermal/structural analysis, the tool model was discretized using 11 type quad 4 elements [26]. Material properties for this type of analysis were taken from the material base of the Marc/Mentat program for steel grade C45. The relationship between specific heat and temperature introduced in the calculations is presented on the graph (Fig. 11), while between thermal conductivity and the temperature of the heated material on the graph (Fig. 12).

Numerical calculations were made assuming that the surface of the tool where the beam of light from the hardening laser light falls heats at a constant speed of 500°C/s. Heating is carried out until hardening temperature (860°C) is reached on surfaces adjacent to the corner at a depth corresponding to the depth of the hardened layer. The simulations were carried out using different values of the k parameter. The calculated temperature distribution for three examples of the k parameter values (0, 1.28 and 1.55) mm are shown in Figure 13. As the analysis shows, the temperature field distributions in individual areas which should be clearly toughened, clearly depend on the k parameter. When using k = 0 mm (Fig. 13 a) it can be seen that the depth of the

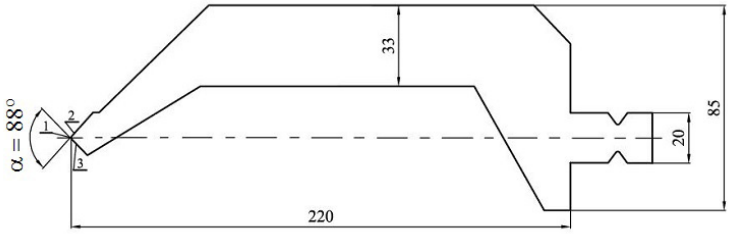

Fig. 10. Shape and dimensions of the tested punch: 1 – corner with a radius r = 0.8 mm, 2, 3 – surfaces adjacent to the corner, α = 88°

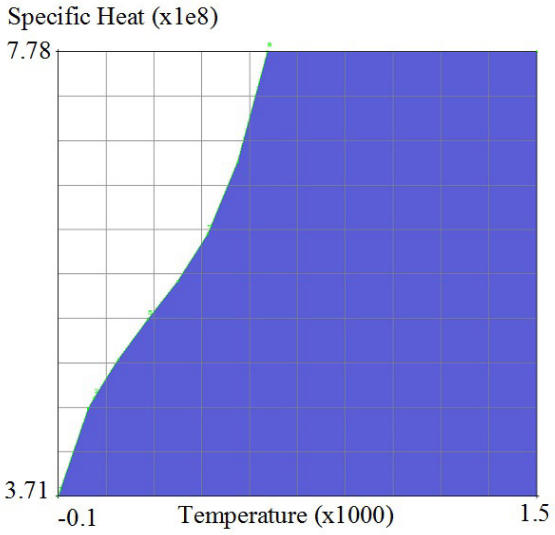

Fig. 11. Relationship between specific heat and tool material temperature

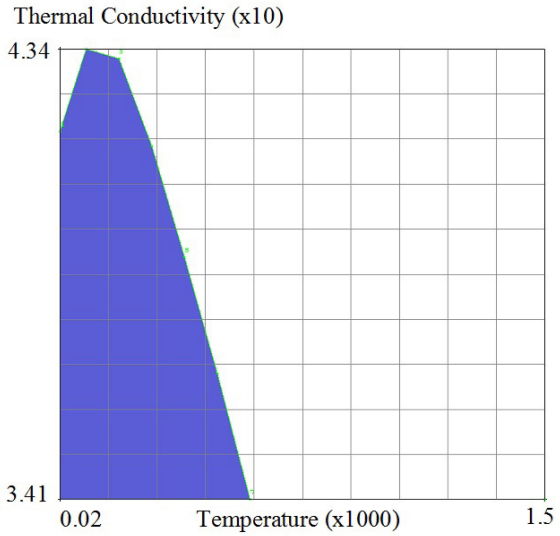

Fig. 12. Relationship between thermal conductivity and tool material temperature

layer heated to the hardening temperature varies. The greatest depth occurs at the corner, while the smallest on the side surfaces the furthest from the corner. This temperature distribution is unfavorable for two reasons. First of all, the corners of tools with small cross-sections will be hardened at a considerable depth throughout, which is disadvantageous, as with variable working loads of the tool, cracks and fragments of brittle material in the corner may appear. Secondly, the properties of the hardened layer depend on the cooling rate. In the case of laser hardening, cooling occurs primarily as a result of heat transfer deep into the material. Thus, the greater the volume of material under the surface of the hardened material layer, the more preferably. In the analyzed case (Fig. 13 a), due to the temperature distribution and volume of material under the corner, the cooling rate will be the smallest, which in turn will cause the hardness of hardened surfaces to be different. The smallest hardness will be on the corner surface, and the highest on the side surfaces adjacent to it. With a properly selected value of the k parameter (in the analyzed case k = 1.28 mm), the depth of the layer heated to the hardening temperature on the corner surface is comparable to the depth of this layer on the side surfaces (Fig. 13 b). In this case, the tool tip heats up as a result of heat transfer from adjacent heated areas. Such an even distribution of hardening temperature on all surfaces ensures comparable properties of the material in the hardened layer including hardness. Importantly, in this case (Fig. 13 b), the tool nose tip will not be hardened through, but at a comparable depth as on the side surfaces. In the case when the value of the k parameter is too high (in the analyzed case k = 1.55 mm), the amount of heat transferred from the adjacent heated layers to the corner is too small, which results in the corner surface not achieving the required hardening temperature (Fig. 13 c). Thus, if the value of parameter k is too high, the material on the corner surface will not harden or more likely will not achieve the required hardness.

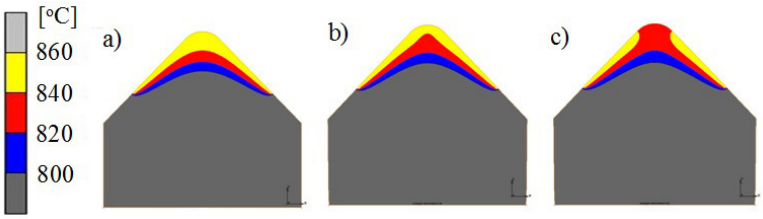

Fig. 13. Effect of the k parameter on the temperature distribution in the hardening area: a) k = 0, b) k=1.28, c) k=1.55

CONCLUSIONS

The revealed microstructure of samples and hardness measurements after laser and induction hardening showed that in the case of laser hardening in the surface area there was a martensitic structure at a relatively small depth. In the case of induction hardening, the martensitic structure occurred at a much greater depth. However, the large depth of the martensitic layer is not desirable due to the fragility of the material. Too large hardened depth is particularly unfavorable in the case of small tool cross-sections, especially their sharp corners often induction hardened in the entire cross-section. This can lead to the formation of cracks already during the hardening of the bending tool, as well as in its operating conditions under the action of variable loads.

It was also shown that the method of laser hardening of the surface of the outer corner of the tool had a significant impact on the properties of the surface layer after hardening. The most preferred of the presented ways of guiding the beam during laser hardening of the surface of the outer corners is the method using a laser beam divider. The effectiveness of this method depends, however, on the proper selection of the k parameter, and it was established that:

1. If the value of the k parameter is too low (in the examined case below 1.28) due to the temperature distribution, the material surface at the corner tip will be hardened at a greater depth than on the side surfaces adjacent to it. In addition, the cooling speed at the top of the corner will be smaller than on adjacent surfaces, which may result in different surface hardness after hardening.
2. If the value of the k parameter is too high (in the examined case above 1.28) due to the temperature difference in the area of hardened surfaces, the material at the corner tip will not obtain the required hardness, and the material layer after hardening will not be homogeneous.
3. With a properly selected value of the k parameter, the distribution of hardening temperature in the hardened layer is evenly distributed over the entire thickness of this layer, both in the corner of the tool and the surfaces adjacent to it. In this case, the use of a beam splitter allows in one pass of the laser head to obtain a homogeneous layer hardened both on the corner surface and surfaces adjacent to it.

In engineering practice, the optimal value of the k parameter can be determined on the basis of numerical simulation results of the heating process or experimentally.

REFERENCES

1. Telasang G., Dutta Majumdar J., Padmanabham G., Manna I. Structure–property correlation in laser surface treated AISIH13 tool steel for improved mechanical properties. Materials Science&Engineering A 2014; 599: 255-267. https://doi.org/10.1016/j.msea.2014.01.083
2. Lee J.H, Jang J.H, Joo B.D, Son Y.M, Moon YH. Laser surface hardening of AISI H13 tool steel. Transactions of Nonferrous Metals Society of China 2009; 19(4): 917-920. https://doi.org/10.1016/S1003-6326(08)60377-5
3. Karamimoghadama M., Moradia M., Azamib M. A comparative investigation of different overlaps of the diode laser hardening in low-carbon steel and stainless steel. Optik 2022; 251(2):168093. https://doi.org/10.1016/j.ijleo.2021.168093
4. Cordovilla F., García-Beltrán A., Sancho P., Domínguez J., Ruiz-de-Lara L., Ocaña J.L. Numerical/experimental analysis of the laser surface hardening with overlapped tracks to design the configuration of the process for Cr-Mo steels. Materials and Design 2016; 102: 225-237. https://doi.org/10.1016/j.matdes.2016.04.038

5. Slatter T., Taylor H., Lewis R., King P. The influence of laser hardening on wear in the valve and valve seat contact. Wear 2009; 267(5-8): 797-806. https://doi.org/10.1016/j.wear.2009.01.040
6. Sugarova J., Sugar P., Frncik M., Necpal M. Moravcikova J., Kusy M. The Influence of the tool surface texture on friction and the surface layers properties of formed component. Advances in Science and Technology Research Journal 2018; 12(1): 181–193. https://doi.org/10.12913/22998624/85704
7. Ready A. Effect of high power radiation. Academic Press, 1971.
8. Mazumder J. Laser Heat Treatment: The State of the Art. Journal of Metals 2013; 35(5): 18-26. https://doi.org/10.1007/BF03338273
9. Aragawa M.E., Gärtnerb E., Schubertab A. Combined laser hardening and laser surface texturing forming tool 1.2379. Procedia CIRP 2020; 94: 914-918. https://doi.org/10.1016/j.procir.2020.09.072
10. Kennedy E., Byrne G., Collins D.N. A review of the use of high power diode lasers in surface hardening. Journal of Materials Processing Technology 2004; 155–156: 1855-1860. https://doi.org/10.1016/j.jmatprotec.2004.04.276
11. Steen W.M., Mazumder J. Laser Material Processing. Springer-Verlag, 2010.
12. Ion J.C. Surface hardening. Laser processing of engineering materials. Principles, procedure and industrial application. Elsevier Butterworth-Heinemann, 2005.
13. Meijer J., Sprang van I. Optimization of laser beam transformation hardening by one single parameter. CIRP Annals 1991; 40: 183-186. https://doi.org/10.1016/S0007-8506(07)61963-5
14. Kou S., Sun D.K. and Le Y.P. A fundamental-study of laser transformation hardening. Metallurgical Transactions A 1983; 14: 643-653. http://dx.doi.org/10.1007/BF02643780
15. Komanduri R., Hou Z.B. Thermal analysis of the laser surface transformation hardening process. International Journal of Heat and Mass Transfer 2001; 44: 2845-2862. https://doi.org/10.1016/S0017-9310(00)00316-1
16. Leung M.K.H., Man H.C., J.K. Yu. Theoretical and experimental studies on laser transformation hardening of steel by customized beam. International Journal of Heat and Mass Transfer 2007; 50: 4600-4606. https://doi.org/10.1016/j.ijheatmasstransfer.2007.03.022
17. Fortunato A., Ascari A., Liverani E., Orazi L.,Cuccolini G. A comprehensive model for laser hardening of carbon steels. Journal of Manufacturing Science Engineering 2013; 135(6): 061002. https://doi.org/10.1115/1.4025563
18. Anusha E., Kumar A., Shariff S. M. Finite element analysis and experimental validation of high-speed laser surface hardening process. The International Journal of Advanced Manufacturing 2021; 115(1): 2403–2421. https://doi.org/10.1007/s00170-021-07303-z
19. Martinez S., Lamikiz A., Ukar E., Tabernero I., Arrizubieta I. Control loop tuning by thermal simulation applied to the laser transformation hardening with scanning optics process. Applied Thermal Engineering 2016; 98: 49-60. https://doi.org/10.1016/j.applthermaleng.2015.12.037
20. Lambiase F., Di Ilio A.M., Paoletti A. Prediction of laser hardening by means of neural network. Procedia CIRP. 2013; 12: 181-186. https://doi.org/10.1016/j.procir.2013.09.032
21. Knap M., Falkus J., Rozman A., Konopka K., Lamut J. The prediction of hardenability using neural networks. Archives of Metallurgy and Materials 2014; 59: 133-136. https://doi.org/10.2478/amm-2014-0021
22. Sehyeok O., Hyungson K. Prediction of hardness and deformation using a 3-D thermal analysis in laser hardening of AISI H13 tool steel. Applied Thermal Engineering 2017; 121: 951-962. https://doi.org/10.1016/j.applthermaleng.2017.04.156
23. Mosavi A., Salehi F., Nadaie L., Karoly S., Gorji N. E. Modeling the temperature distribution during laser hardening process, Results in Physics 2020; 16: 102883. https://doi.org/10.1016/j.rinp.2019.102883
24. http://www.plasmet.net
25. Kut S., Kogut K. Method for laser hardening of tools, with splitting the laser light. Polish Patent No. Pat233215, 2016.
26. MSC Software: MSC. Marc Volume B: Element Library, Version 2010.